# Novel Strategies for Genomic Manipulation of *Trichoderma reesei* with the Purpose of Strain Engineering

Christian Derntl, Daniel P. Kiesenhofer, Robert L. Mach, Astrid R. Mach-Aigner

Department for Biotechnology and Microbiology, Institute of Chemical Engineering, TU Wien, Vienna, Austria

The state-of-the-art procedure for gene insertions into *Trichoderma reesei* is a cotransformation of two plasmids, one bearing the gene of interest and the other a marker gene. This procedure yields up to 80% transformation efficiency, but both the number of integrated copies and the loci of insertion are unpredictable. This can lead to tremendous pleiotropic effects. This study describes the development of a novel transformation system for site-directed gene insertion based on auxotrophic markers. For this purpose, we tested the applicability of the genes *asl1* (encoding an enzyme of the L-arginine biosynthesis pathway), the *hah1* (encoding an enzyme of the L-lysine biosynthesis pathway), and the *pyr4* (encoding an enzyme of the uridine biosynthesis pathway). The developed transformation system yields strains with an additional gene at a defined locus that are prototrophic and ostensibly isogenic compared to their parental strain. A positive transformation rate of 100% was achieved due to the developed split-marker system. Additionally, a double-auxotrophic strain that allows multiple genomic manipulations was constructed, which facilitates metabolic engineering purposes in *T. reesei*. By employing *goxA* of *Aspergillus niger* as a reporter system, the influence on the expression of an inserted gene caused by the orientation of the insertion and the transformation strategy used could be demonstrated. Both are important aspects to be considered during strain engineering.

The filamentous ascomycete *Trichoderma reesei* (teleomorph, *Hypocrea jecorina*) (1) is of industrial interest due to its outstanding secretory capacities. As a saprophyte, it naturally secretes large amounts of cellulases and hemicellulases. The most abundantly secreted and industrially relevant enzymes are the two main cellobiohydrolases, CBHI and CBHII (EC 3.2.1.91) (2). *T. reesei* cellulases find use in a wide range of industrial applications, such as the paper and pulp, textile, and food and feed industries (3), and they are a crucial factor for cost-effective production of cellulose ethanol (4). Yields of over 100 g/liter of cellulases can be achieved in industry-scale production (5). These secretion rates are unique and make *T. reesei* an attractive candidate as host for heterologous protein production.

*T. reesei* has been a target of basic and applied research in regard to its regulatory mechanisms of cellulase and hemicellulase gene expression (6–13), secretion pathways (14), sexual development (15), and light response (16). Nearly all of these investigations were performed in the wild-type strain QM6a (ATCC 13631) or the mutant strain QM9414 (ATCC 26921). Both strains can be transformed using different techniques, such as polyethylene glycol (PEG)-mediated transformation of protoplasts (17), particle bombardment (18), electroporation (19), and *Agrobacterium tumefaciens*-mediated transformation (20).

Over the years there have been reports on ongoing attempts to increase the number of available marker genes, e.g., *bar* (phosphinothricin resistance) (21), *ble* (bleomycin/phleomycin resistance) (22), *ben* (benomyl resistance) (23), *ptrA* (pyrithiamine resistance) (24), the dominant-nutritional marker *suc1* (sucrose utilization) (25), the auxotrophic markers *argB* (ornithine transcarbamylase) (17) and *pyr2* (orotate phosphoribosyltransferase) (26), and *hxk1* (hexokinase) (27). However, only a few turned out to be applicable for common use, namely, *hph* (hygromycin B resistance) (28), *pyr4* (orotidine 5′-phosphate decarboxylase) (29), and *amdS* (utilization of acetamide) (17). Three of them have the additional advantage of being bidirectionally selectable; i.e., *amdS* is negatively selectable on fluoroacetamide (30), and

*pyr4* and *pyr2* are negatively selectable on 5-fluoorotic acid (5-FOA) (26, 29).

Cotransfomation of two plasmids, one bearing the marker gene and the other containing the gene of interest, is a commonly used method for gene insertions in *T. reesei*. In 80% of the cases the gene of interest is integrated into the genome of *T. reesei* randomly and in variable copy numbers (17). This is problematic for different reasons. First, successful integration of the marker gene (and positive selection) does not ensure integration of the gene of interest. Second, the untargeted insertion can provoke an unpredictable locus effect. Third, the resulting copy number is not controllable. Therefore, this technique demands a laborious subsequent investigation of a number of (positively) transformed strains.

A way to overcome this problem is site-specific integration. For this purpose, a prerequisite is high efficiency of homologous inte-

**TABLE 1** Strains used in this study

| Strain | Phenotype[a] | | | |
|---|---|---|---|---|
| | Hygromycin B | 5-FOA/uridine | Arginine | Lysine |
| QM6a Δ*tmus53* | | | | |
| QM6a Δ*tmus53* Δ*pyr4* | | R/A | | |
| QM6a Δ*tmus53*/*eyfp* (in *pyr4* locus) | | | | |
| QM6a Δ*tmus53* Δ*asl1* | R | | A | |
| QM6a Δ*tmus53*/*eyfp* (in *asl1* locus) | | | | |
| QM6a Δ*tmus53* Δ*hah1* | R | | | A |
| QM6a Δ*tmus53* Δ*pyr4* Δ*asl1* | R | R/A | A | |
| QM6a Δ*tmus53*/pc2G-FW (in *pyr4* locus) | | | | |
| QM6a Δ*tmus53* Δ*pyr4*/pc2G-FW (in *pyr4* locus) | | R/A | | |
| QM6a Δ*tmus53* Δ*pyr4*/pc2G-RV (in *pyr4* locus) | | R/A | | |

[a] R, resistance; A, auxotrophy.

gration, an obstacle that has recently been overcome by deletion of genes involved in the nonhomologous end-joining mechanism. Gene targeting in a TU6 Δ*tku70* strain and a QM6a Δ*tmus53* strain turned out to be highly efficient, with homologous integration rates of up to 100% depending on the integration site (19, 21). These systems were developed in particular for (serial) deletions of a gene (see, e.g., reference 21). Based on a QM6a Δ*tku70* Δ*pyr2* strain, Jørgensen et al. constructed a site-specific integration system in which the gene of interest is inserted at the *ade2* locus together with *pyr2* used as marker (26). However, this transformation system yields strains which are adenine auxotrophic and nonisogenic compared to the parental strain.

In this study, we aimed to develop a labor-saving transformation strategy that is in particular useful for gene insertions with the aim of strain engineering. This demands a system that yields (i) exclusively positively transformed strains, (ii) prototrophic strains for simple subsequent handling, and (iii) strains which are isogenic compared to the parental strain for subsequent investigations in a correct genetic background. For this purpose, we investigated the applicability of novel auxotrophy/prototrophy-based marker genes, namely, genes coding for the argininosuccinate lyase and the homoaconitate hydratase. We constructed strains bearing truncated versions of these two genes and a *pyr4* deletion strain in a QM6a Δ*tmus53* background. The obtained strains were tested for their usability as recipient strains in a transformation procedure selecting for prototrophic strains. Partial deletion of the marker genes should ensure that prototrophy is regained only if the integration occurs at the correct locus, leading to a reestablishment of the full marker gene. The basic concept of such a split-marker system is schematically displayed in Fig. S1 in the supplemental material. The received strains are ostensibly isogenic compared to their parental strain. As an example, we demonstrated the proper functioning of this site-directed integration strategy by inserting an enhanced yellow fluorescent protein (EYFP) gene expression cassette in the investigated loci. Additionally, a double-deletion (double-auxotrophic) strain that can be used in the same way as the single-deletion strains but allows multiple genomic manipulation steps was constructed. Because for strain engineering purposes the strength of expression of the target gene is crucial, we finally assessed the influence of orientation of the insertion and the applied transformation strategy on target gene expression by using a *goxA* reporter system.

## MATERIALS AND METHODS

**Strains and cultivation conditions.** *T. reesei* strains QM6a Δ*tmus53* (21), QM6a Δ*tmus53* Δ*pyr4* (this study), QM6a Δ*tmus53*Δ*asl1* (this study), QM6a Δ*tmus53* Δ*hah1* (this study), QM6a Δ*tmus53* Δ*pyr4* Δ*asl1* (this study), QM6a Δ*tmus53*/pc2G-FW (this study), QM6a Δ*tmus53* Δ*pyr4*/pc2G-FW (this study), and QM6a Δ*tmus53* Δ*pyr4*/pc2G-RV (this study) were maintained on malt extract (MEX) agar at 30°C. If applicable, uridine, L-arginine, L-lysine, 5-FOA, and hygromycin B were added to final concentrations of 5 mM, 2.5 mM, 4 mM, 1.5 mg/ml, and 113 U/ml, respectively. Mandels-Andreotti (MA) medium (31) without peptone containing 1% glycerol and 1% D-glucose was used as minimal medium. Table 1 lists all strains used and their phenotypes (resistance and auxotrophy).

For carbon source replacement experiments, mycelia were precultured in 250 ml of MA medium supplemented with 1% (wt/vol) glycerol as the sole carbon source on a rotary shaker (180 rpm) at 30°C for 24 h. A total of $10^9$ conidia per liter (final concentration) were used as the inoculum. Pregrown mycelia were washed, and equal amounts were resuspended in 20 ml MA medium containing 1.5 mM sophorose as the sole carbon source and were incubated for 5 and 8 h. Culture supernatant samples were derived from biological duplicates.

*Escherichia coli* strain Top10 (Invitrogen, Life Technologies, Paisley, United Kingdom) was used for all cloning purposes throughout this study and maintained on LB at 37°C. If applicable, ampicillin, spectinomycin, or hygromycin B was added to a final concentration of 100 mg/ml, 100 mg/ml, or 113 U/ml, respectively.

**Plasmid constructions.** PCRs for cloning purposes were performed with Phusion high-fidelity DNA polymerase (Thermo Scientific, Waltham, MA, USA) according to the manufacturer's instructions. All primers used are listed in Table S1 in the supplemental material. Nucleic acid sequences and a detailed construction description for each plasmid are provided in the supplemental material.

For the construction of pCD-Δpyr4, the 5′ flank and the terminator sequence of *pyr4* were inserted into pJET1.2 (Thermo Scientific) (see Fig. S2 in the supplemental material). For the construction of pCD-Δasl1, a hygromycin resistance cassette was inserted between the 5′ and 3′ flanking regions of *asl1* into a derivative of pMS (Life Technologies) (see Fig. S3 in the supplemental material). For the construction of pCD-Δhah1, a hygromycin resistance cassette was inserted between the 5′ and 3′ flanking regions of *hah1* into pJET1.2 (Thermo Scientific) (see Fig. S4 in the supplemental material). For the construction of pCD-RPyr4, the complete *pyr4* locus was inserted into a derivative of pMS (Life Technologies) (see Fig. S5 in the supplemental material). For the construction of pCD-RPyr4T, the terminator of *cbh2* was inserted into pCD-RPyr4 downstream the 5′ flank of *pyr4* (see Fig. S5 in the supplemental material). For the construction of pCD-RAsl1, the complete *asl1* locus was inserted into a derivative of pMS (Life Technologies) (see Fig. S6 in the supplemental
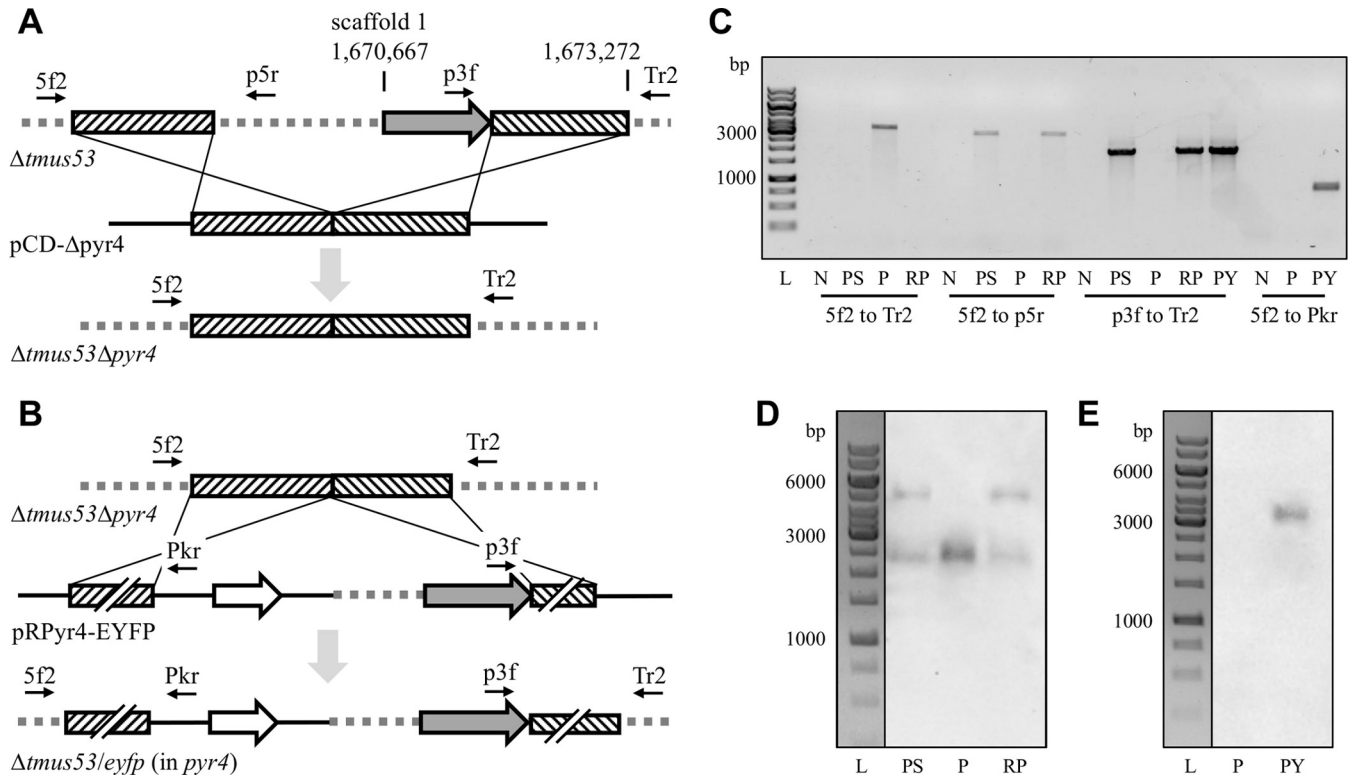
**FIG 1** Modification of the *pyr4* locus during strain generation. (A and B) Schematic drawings of the destruction of the *pyr4* locus in the parental strain QM6a Δ*tmus53* (Δ*tmus53*) by homologous recombination with the plasmid pCD-Δpyr4, yielding a *pyr4* deletion strain (Δ*tmus53*Δ*pyr4*) (A), and integration of the EYFP gene expression cassette upstream of *pyr4* by recombination with the plasmid pRPyr4-EYFP, yielding a reestablished strain additionally bearing the EYFP gene [Δ*tmus53*/*eyfp* (in *pyr4*)] (B). The position of the *pyr4* locus on scaffold 1 is indicated at the top. Thin black arrows indicate the approximate positions of the primers used for genomic characterization via PCR and subsequent sequencing. 5f2, 5pyr4_fwd2; p5r, pyr4_5rev; p3f, pyr4_3f; Tr2, Tpyr4_rev2; Pkr, Ppki_Mrev. Black-rimmed gray arrows represent the *pyr4* gene, hatched boxes represent flanking regions for homologous recombination, gray arrows indicate homologous recombination events, black-rimmed white arrows represent the EYFP gene, gray dotted lines represent genomic DNA sequences, and solid black lines represent plasmid DNA sequences. (C to E) Correct and exclusive integration events at the *pyr4* locus were verified by PCR (C) and Southern blot analyses (D and E). (D) Southern blot analysis of BcuI-digested chromosomal DNA using the flanking regions as probes resulted in expected signals at bp 2469 and 5297 for the parent locus or at bp 2326 and 2500 for the modified locus. (E) Southern blot analysis of AatII-digested chromosomal DNA using the EYFP gene coding region as probe resulted in an expected signal at bp 3289. L, 1-kb DNA ladder; N, no-template control; PS, QM6a Δ*tmus53*; P, QM6a Δ*tmus53* Δ*pyr4*; RP, reestablished QM6a Δ*tmus53* (obtained via transformation with pCD-RPyr4); PY, QM6a Δ*tmus53*/*eyfp*.

material). For the construction of pCD-EYFP, the codon-optimized gene coding for EYFP was put under the control of the constitutive *pki* promoter upstream of the *cbh2* terminator in pRLM$_{ex}$30 (28) (see Fig. S7 in the supplemental material). For the construction of pRPyr4-YFP and pRAsl1-YFP, a PCR product was created with primers Ppki_fwd_Kpn2I and Tcbh2_rev-BcuI using pCD-EYFP as the template, which was digested with Kpn2I and BcuI, and inserted into pCD-RPyr4 (digested with the same enzymes) or into pCD-Rasl1 (digested with Kpn2I and NheI), resulting in pRPyr4-EYFP and pRAsl1-EYFP, respectively. For the construction of pRPyr-pc2G-FW, the *goxA* gene was fused to the *cbh2* promoter and inserted into pCD-RPyr4T (see Fig. S8 in the supplemental material). For the construction of pDelp4-pc2G-FW, the *goxA* gene together with its own terminator was fused to the *cbh2* promoter (see Fig. S9 in the supplemental material). The expression cassette was inserted into pCD-Δpyr4 in forward orientation. For the construction of pDelp4-pc2G-RV, the *goxA* gene together with its own terminator was fused to the *cbh2* promoter (see Fig. S10 in the supplemental material). The expression cassette was inserted into pCD-Δpyr4 in reverse orientation.

**Fungal transformation.** The protoplast transformation of *T. reesei* was performed as described by Gruber et al. (29). Typically, 30 to 50 μg of digested plasmid DNA (in 15 μl sterile double-distilled water [ddH$_2$O]) was used for transformation of 10$^7$ protoplasts (in 200 μl).

For selection for resistance against 5-FOA and hygromycin B, 100 μl to 2 ml of the transformation reaction mixture was added to 10 ml melted, 50°C warm MEX agar containing 1.2 M sorbitol. This mixture was poured into sterile petri dishes and incubated at 30°C for 5 h after solidification. Subsequently, 10 ml melted, 50°C MEX agar containing 1.2 M sorbitol and a double concentration of 5-FOA or hygromycin B was poured on top of the protoplast-containing layer. Plates were incubated at 30°C for 2 to 5 days until colonies were visible. For selection for prototrophy, 100 μl to 2 ml of the transformation reaction mixture was added to 20 ml melted, 50°C warm minimal medium agar containing 1.2 M sorbitol and, in the case of *asl1* back transformation, additionally 0.25 mM L-arginine. This mixture was poured into sterile petri dishes and after solidification was incubated at 30°C for 3 to 7 days until colonies were visible.

**Isolation of chromosomal DNA and PCR screening.** Chromosomal DNA was isolated from mycelium by grinding in liquid nitrogen followed by a phenol-chloroform extraction (29). RNA was degraded using RNase A (Thermo Scientific). DNA was precipitated with isopropanol, washed with 70% ethanol, and dissolved in ddH$_2$O. For testing the genotype, 10 ng of chromosomal DNA was used as the template in a 25-μl PCR mixture using GoTaq G2 polymerase (Promega, Madison, WI, USA) according to the manufacturer's instructions. All primers used are listed in Table S1 in the supplemental material. For subsequent agarose gel electrophoresis of
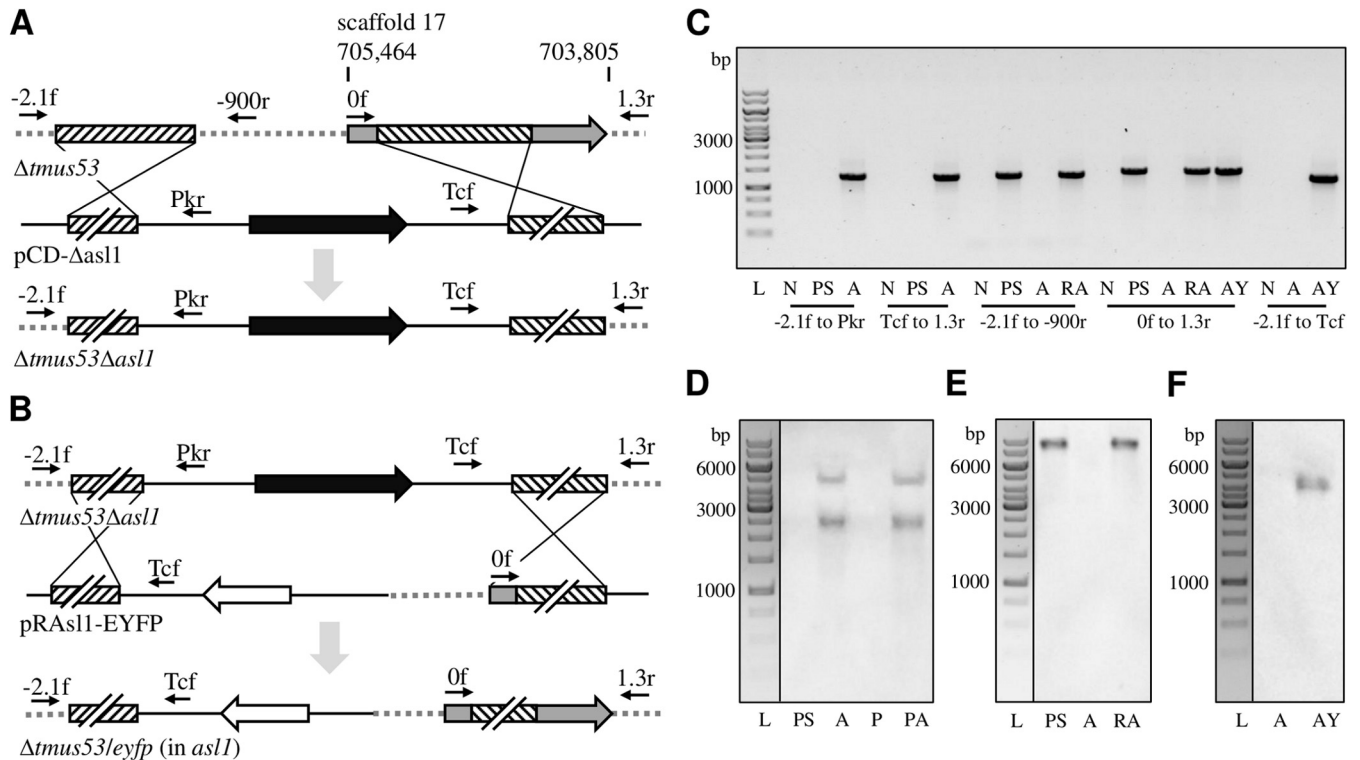
**FIG 2** Modification of the *asl1* locus during strain generation. (A and B) Schematic drawings of the partial deletion of *asl1* in the parental strain QM6a Δ*tmus53* (Δ*tmus53*) by homologous recombination with the plasmid pCD-Δasl1, yielding an *asl1* deletion strain (Δ*tmus53* Δ*asl1*) (A), and integration of the EYFP gene expression cassette upstream of *asl1* by recombination with the plasmid pRAsl1-EYFP, yielding a reestablished strain additionally bearing the EYFP gene [Δ*tmus53*/*eyfp* (in *asl1*)] (B). The position of the *asl1* locus on scaffold 17 is indicated at the top. Thin black arrows indicate the approximate positions of the primers used for genomic characterization via PCR and subsequent sequencing. −2.1f, asl1-2.1kf; −900r, asl1-900r; 0f, asl1_0f; Pkr, Ppki_Mrev; Tcf, Tcbh2Mfwd. Black-rimmed gray arrows represent the *asl1* gene, hatched boxes represent regions for homologous recombination, thick black arrows represent the *hyg* gene, gray arrows indicate homologous recombination events, black-rimmed white arrows represent the EYFP gene, gray dotted lines represent genomic DNA sequences, and solid black lines represent plasmid DNA sequences. (C to E) Correct and exclusive integration events at the *asl1* locus were verified by PCR (C) and Southern blot analyses (D and E). (D) Southern blot analysis of PstI-digested chromosomal DNA using the *hph* coding region as probe resulted in expected signals at bp 2432 and 5040. (E) Southern blot analysis of NsiI-digested chromosomal DNA using the deleted promoter of *asl1* as a probe resulted in an expected signal at bp 9999. (F) Southern blot analysis of EcoRI-digested chromosomal DNA using the EYFP gene coding region as a probe resulted in an expected signal at bp 4035. L, 1-kb DNA ladder; N, no-template control; PS, QM6a Δ*tmus53*; A, QM6a Δ*tmus53*Δ*asl1*; RA, reestablished QM6a Δ*tmus53* (via transformation with pCD-RAsl1); AY, QM6a Δ*tmus53*/*eyfp*; P, QM6a Δ*tmus53*Δ*pyr4*; PA, QM6a Δ*tmus53* Δ*pyr4* Δ*asl1*.

DNA fragments, a GeneRuler 1-kb DNA ladder (Thermo Scientific) was applied for estimation of fragment size. DNA sequencing was performed at Microsynth (Balgach, Switzerland).

**Southern blot analysis.** Fifteen micrograms of chromosomal DNA was digested with 30 U of the indicated restriction enzymes. The resulting DNA fragments were separated by electrophoresis on an 0.8% agarose gel, denatured in 0.4 M NaOH, and transferred by capillary force onto a Biodyne B 0.45-μm nylon membrane (Pall Corporation, Port Washington, NY, USA) using 10× SSC (1× SSC is 0.15 M NaCl plus 0.015 M sodium citrate). A 1.5-μg quantity of biotinylated DNA probe was used for hybridization at 65°C overnight. Labeling of the probe was performed by using Klenow fragment (exo−) (Thermo Scientific), random hexamer primers, and biotin-11-dUTP (Jena Bioscience, Jena, Germany). Signals were visualized by using poly-horseradish peroxidase (poly-HRP) conjugated to streptavidin and ECL Plus Western blotting substrate (both from Thermo Scientific Pierce, Life Technologies) on a ChemiDoc MP (Bio-Rad Laboratories, Hercules, CA, USA).

**Biolog microarray technique.** The global carbon assimilation profiles were evaluated by using a Biolog FF MicroPlate (Biolog, Inc., Hayward, CA) following a protocol described before (32) with minor modifications; the inoculum was prepared from cultivations on MEX plates incubated at

30°C. Mycelial growth was measured after 18, 24, 30, 36, 42, 48, 66, 72, and 90 h in biological triplicates.

**Live-cell imaging.** *T. reesei* strains were incubated on solid rich-medium agar for 2 days, and mycelium for microscopy was prepared using the "inverted agar block" method (33). Live-cell imaging was performed using a Nikon C1 confocal laser scanning unit mounted on a Nikon Eclipse TE2000-E inverted microscope base (Nikon GmbH, Vienna, Austria). A Nikon Plan Apo VC 60×/1.2 water immersion objective lens was used. EYFP was excited with the 488-nm laser line of an argon ion laser. The emitted fluorescence was separated by a Nikon MHX40500b/C100332 filter cube and detected with a photomultiplier tube within the range of 500 to 530 nm. Bright-light images were captured simultaneously with a Nikon C1-TD transmitted light detector mounted behind the condenser turret.

**Glucose oxidase assay.** The glucose oxidase activity was assayed as described previously (34) using ABTS [2,2′-azino-di-(3ethyl-benzthiazoline sulfonate)] (Molekula Ltd., Gillingham, United Kingdom) and horseradish peroxidase (Sigma-Aldrich). One unit of activity is defined as the amount of enzyme that oxidizes 1 μmol of D-glucose per min at pH 5.8 and 25°C. Measurements were carried out in technical triplicates. For the

reference to the biomass, the mycelium was separated from the culture supernatant by filtration using Miracloth and dried at 80°C overnight.

## RESULTS

**Identification of novel marker genes for transformation of *T. reesei*.** The exploitation of auxotrophy/prototrophy is an obviously advantageous system because it avoids the application of heterologous genes and is reversible. Therefore, we searched for genes that were previously shown to cause auxotrophy in *Aspergillus* spp. An additional requirement for potential marker genes was that the neighboring genes (located upstream or downstream) are at least a distance of 3 kb to avoid any undesired locus effects. For the *in silico* analysis we used the *T. reesei* genome database (http://genome.jgi-psf.org/Trire2/Trire2.home.html) and found that the homologs of the *A. niger argH* (coding for the argininosuccinate lyase [EC 4.3.2.1]) (35) and *A. nidulans lysF* (coding for the mitochondrial homoaconitate hydratase [EC 4.2.1.36]) (36) fulfilled these criteria. The argininosuccinate lyase (EC 4.3.2.1) catalyzes the reversible reaction from *N*-(ʟ-)arginosuccinate to fumarate and ʟ-arginine, which is an essential step in the urea cycle and links it to the citric acid cycle (see Fig. S11A in the supplemental material). In *T. reesei*, the gene encoding the argininosuccinate lyase (protein ID 80268) is located at scaffold 17:703805-705613 and is in this report termed *asl1*. The mitochondrial homoaconitate hydratase (EC 4.2.1.36) is part of the fungus-specific alpha-aminoadipate pathway for ʟ-lysine biosynthesis and catalyzes the reversible reaction from homoisocitrate to *cis*-homoaconitate and $H_2O$ (see Fig. S11B in the supplemental material). The gene encoding the mitochondrial homoaconitate hydratase (protein ID 81570) is located at scaffold 25:427291-430204 and is in this report termed *hah1*. The auxotrophic marker *pyr4* also is distant enough from its upstream neighboring gene to be included in our strategy.

**Deletion of *pyr4*, *asl1*, and *hah1* from the QM6a Δ*tmus53* genome.** For the deletion of the genes *pyr4*, *asl1*, and *hah1* from the genome of *T. reesei* QM6a Δ*tmus53*, a double-crossover recombination strategy was applied and is schematically presented in Fig. 1A, 2A, and 3A, respectively. The deletion of *pyr4* yielded three candidates. After one round of homokaryon purification by streaking conidial spores, strains were tested for uridine auxotrophy. One auxotrophic strain (Fig. 4, Δ*pyr4* strain) was chosen for further genomic manipulation. The correct integration of the deletion cassette in this strain was verified by PCR (Fig. 1C) followed by sequencing of the PCR products.

In the case of the partial deletion of *asl1*, we obtained 17 candidates. Six were subjected to four rounds of homokaryon purification by streaking conidial spores and were subsequently tested for arginine auxotrophy. One auxotrophic strain (Fig. 4, Δ*asl1* strain) was chosen for further genomic manipulation. The correct integration of the deletion cassette in this strain was verified by PCR (Fig. 2C) followed by sequencing of the PCR products. Further, this strain was tested for its global carbon utilization in a Biolog assay and turned out not to be able to grow on any of the tested carbon sources (data not shown). This indicates that *T. reesei* cannot circumvent the lack of the *asl1* gene by using other substances as carbon sources.

For the partial deletion of *hah1*, we obtained 22 candidates. Again, six candidates were subjected to four rounds of homokaryon purification by streaking conidial spores. Out of the resulting strains, three had an altered phenotype, i.e., formed more aerial hyphae and secreted an increased amount of a yellow compound on rich medium.
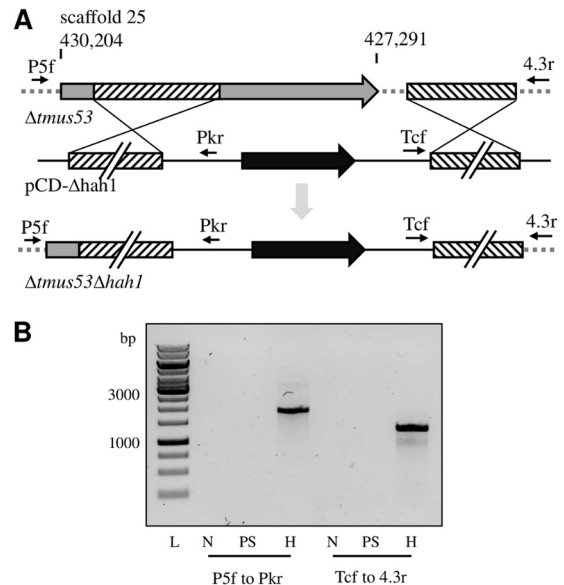


**FIG 3** Modification of the *hah1* locus during strain generation. (A) Schematic drawing of the partial deletion of *hah1* in the parental strain QM6a Δ*tmus53* (Δ*tmus53*) by homologous recombination with the plasmid pCD-Δhah1, yielding a *hah1* deletion strain (Δ*tmus53* Δ*hah1*). The position of the *hah1* locus on scaffold 25 is indicated at the top. Thin black arrows indicate the approximate positions of the primers used for genomic characterization via PCR and subsequent sequencing. P5f, Phah1_5f; 4.3r, hah1 + 4.3kr; Pkr, Ppki_Mrev; Tcf, Tcbh2Mfwd. The black-rimmed gray arrow represents the *hah1* gene, hatched boxes represent regions for homologous recombination, thick black arrows represent the *hyg* gene, the gray arrow indicates a homologous recombination event, gray dotted lines represent genomic DNA sequences, and solid black lines represent plasmid DNA sequences. (B) Agarose gel electrophoresis of DNA fragments obtained by PCR in order to verify genetic modifications within the *hah1* locus. L, 1-kb DNA ladder; N, no-template control; PS, QM6a Δ*tmus53*; H, QM6a Δ*tmus53* Δ*hah1*.

The correct integration of the deletion cassette in these strains was verified by PCR (one example is shown in Fig. 3B) and subsequent sequencing of the PCR products. Surprisingly, the growth of the obtained strains on minimal medium was unchanged compared to that of the parental strain (Fig. 4, Δ*hah1* strain [mycelium]). Only the strains with the altered phenotype could not germinate on minimal medium when small amounts of spores were used as the inoculum instead of mycelium (Fig. 4, Δ*hah1* strain [spores]). Because of the observed semiauxotrophy, we additionally tested regeneration of protoplasts and found that they could recover well on minimal selection medium (data not shown). An additional investigation on the global carbon utilization in one *hah1* deletion strain yielded a pattern similar to that for the parental strain (data not shown). Since the deletion of the *hah1* gene did not result in a strain exhibiting a phenotype that can be unambiguously distinguished from its parental strain, we do not recommend the usage of *hah1* as marker in *Trichoderma*.

**Reestablishment of the *pyr4* and *asl1* loci leads to regaining of prototrophy.** We found that the deletion of *pyr4* and *asl1* led to clear auxotrophic phenotypes. Consequently, we aimed to use the corresponding deletion strains as recipient strains in a fungal transformation strategy, which should yield prototrophic strains. Before that, we tested whether the deletion cassettes used for construction of the auxotrophic strains were integrated only once in the genomes by performing Southern blot analyses. The absence
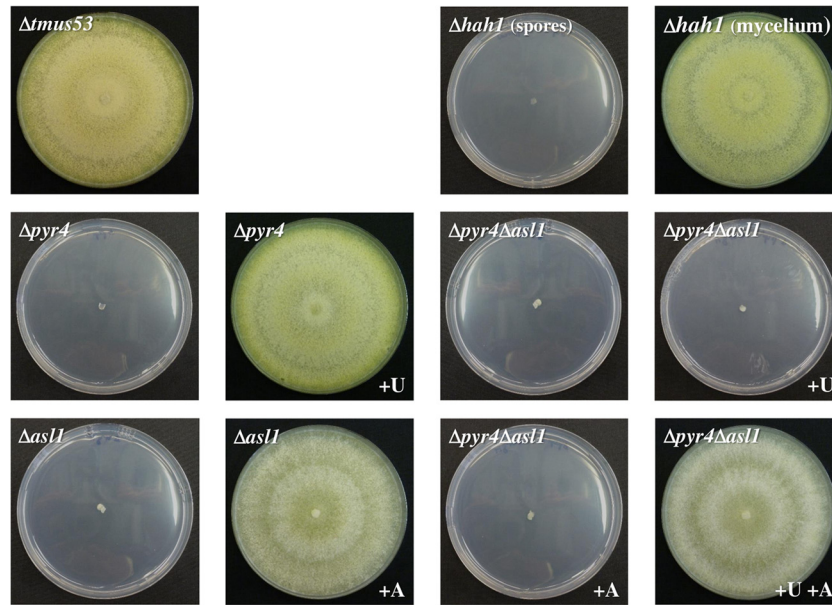
**FIG 4** Effect of deletion of potential marker genes on the growth behavior of *T. reesei*. *T. reesei* strains QM6a Δ*tmus53* (Δ*tmus53*), QM6a Δ*tmus53* Δ*pyr4* (Δ*pyr4*), QM6a Δ*tmus53* Δ*asl1* (Δ*asl1*), and QM6a Δ*tmus53* Δ*pyr4* Δ*asl1* (Δ*pyr4*Δ*asl1*) were inoculated with a piece of mycelium and grown in petri dishes containing minimal medium alone or supplemented with uridine (+U) and/or L-arginine (+A) for 4 days at 30°C. Strain QM6a Δ*tmus53* Δ*hah1* (Δ*hah1*) was inoculated either with spores or a piece of mycelium and grown on minimal medium plates in the same way.

of any ectopically integrated deletion cassettes (Fig. 1D and 2D) allows the usage of the Δ*pyr4* strain and the Δ*asl1* strain as recipient strains. We then needed to investigate whether the reestablishment of the loci indeed causes regain of prototrophy and whether the gained phenotype can be clearly discriminated from that of the auxotrophic parental strain. For the reestablishment of the *pyr4* and the *asl1* loci, we applied double-crossover recombination strategies, which are schematically presented in Fig. 1B and 2B, respectively. Back transformation of *pyr4* resulted in eight candidates, six of which were prototrophic and five of which had the *pyr4* locus reestablished. Correct genomic integration exclusively at the *pyr4* locus was verified by PCR (Fig. 1C) and subsequent sequencing of the PCR products as well as by Southern blotting (Fig. 1D). In the case of *asl1*, we obtained five candidates, four of which were prototrophic. All of them had the *asl1* locus reestablished. Correct genomic integration at the *asl1* locus was verified by PCR (Fig. 2C) and subsequent sequencing of the PCR products as well as by Southern blotting (Fig. 2E). Obviously, the reestablishment of the *pyr4* and *asl1* loci resulted in selectable prototrophy, which is an advantageous aspect of a transformation system. Further, we needed to test whether the integration of an additional gene, which is the actual purpose of the developed system, has an effect on prototrophy.

**Utilization of partial *asl1* as a split-marker system and of *pyr4* for site-specific integration.** To exemplify the utility of the *pyr4* and *asl1* deletion strains, we introduced a gene of interest together with the marker gene in order to see if the finally obtained strain functionally expresses both genes. We used the EYFP gene as the gene of interest because its functional expression is easy to investigate. *T. reesei* QM6a Δ*tmus53*Δ*pyr4* and QM6a Δ*tmus53*Δ*asl1* were transformed with fragments bearing an EYFP gene expression cassette and the respective markers between the corresponding flanking regions. Targeting the EYFP gene expres-

sion cassette into the *pyr4* locus resulted in four candidates, three of which turned out to be prototrophic. Targeting into the *asl1* locus resulted in two candidates, both of which were found to be prototrophic. The exclusive insertion of the EYFP gene expression cassette at the correct loci was determined by PCR (Fig. 1C and 2C) and subsequent sequencing of the PCR products as well as by Southern blotting analyses (Fig. 1E and 2F). All strains with the integrated EYFP gene exhibited the same phenotype as their ancestor *T. reesei* QM6a Δ*tmus53* in regard to growth and sporulation behavior on minimal and rich media (data not shown). Functional expression of the EYFP gene in both loci was confirmed via
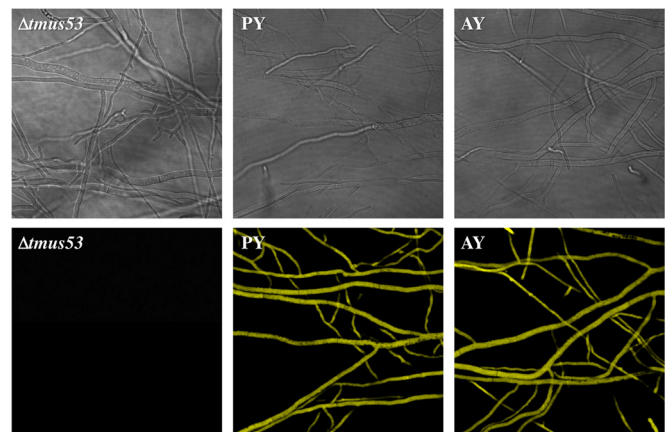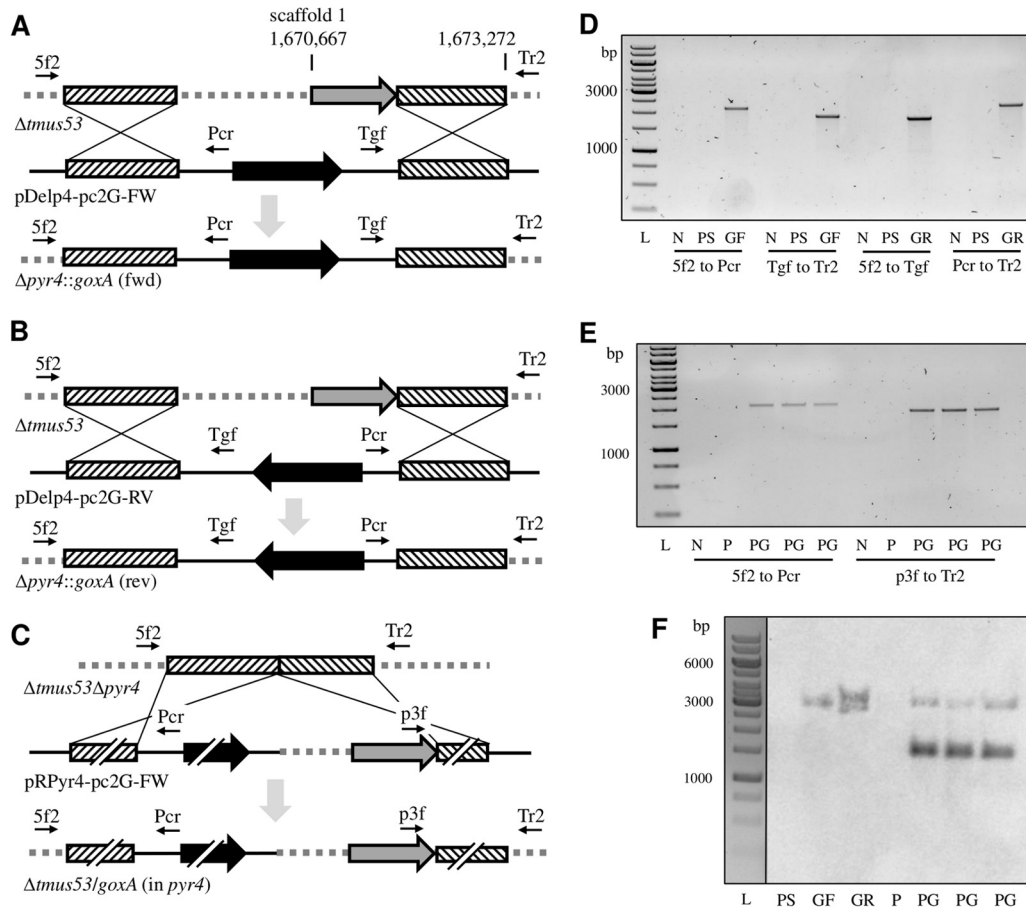


**FIG 5** Microscopic analyses of *T. reesei* strains expressing EYFP. Bright-light (top panels) and fluorescence (bottom panels) live-cell images of QM6a Δ*tmus53* (Δ*tmus53*), QM6aΔ*tmus53*/*eyfp* bearing the EYFP gene expression cassette upstream of *pyr4* (PY), and QM6a Δ*tmus53*/*eyfp* bearing the EYFP gene expression cassette upstream of *asl1* (AY) are shown.

**FIG 6** Modification of the *pyr4* locus for generation of *goxA* expression strains. (A and B) Schematic drawings of the insertion of the *goxA* expression cassette in forward or reverse orientation into the *pyr4* locus of the parental strain QM6a Δ*tmus53* (Δ*tmus53*) by homologous recombination with the plasmid pDelp4-pc2G-FW or pDelp4-pc2G-RV, resulting in the *pyr4* deletion strains QM6a Δ*tmus53* Δ*pyr4*/pc2G-FW [Δ*pyr4*::*goxA*(fwd)] (A) and QM6a Δ*tmus53* Δ*pyr4*/pc2G-RV [Δ*pyr4*::*goxA*(rev)] (B), respectively. (C) Schematic drawing of the insertion of the *goxA* expression cassette into the *pyr4* locus of QM6a Δ*tmus53* Δ*pyr4* (Δ*pyr4*) by homologous recombination with the plasmid pRPyr4-pc2G-FW, resulting in strain QM6a Δ*tmus53*/pc2G-FW [Δ*tmus53*/*goxA* (in *pyr4*)]. The position of the *pyr4* locus on scaffold 1 is indicated at the top. Thin black arrows indicate the approximate positions of the primers used for genomic characterization via PCR and subsequent sequencing. 5f2, 5pyr4_fwd2; Tr2, Tpyr4_rev2; Pcr, pchb2_rev-BamHI-NheI; Tgf, TgoxA_fwd; p3f; pyr4_3f. Black-rimmed gray arrows represent the *pyr4* gene, hatched boxes represent regions for homologous recombination, thick black arrows represent the *goxA* gene, gray arrows indicate homologous recombination events, gray dotted lines represent genomic DNA sequences, and solid black lines represent plasmid DNA sequences. (D to F) Correct and exclusive integration events at the *pyr4* locus were verified by PCR (D and E) and Southern blot analysis (F). (F) Southern blot analysis of SacII-digested chromosomal DNA using the *goxA* coding region as probe resulted in expected signals at bp 3002 and 3006 for QM6a Δ*tmus53* Δ*pyr4*/pc2G-FW, at bp 2817 and 3191 for QM6a Δ*tmus53* Δ*pyr4*/pc2G-RV, and at bp 1496 and 2987 for QM6a Δ*tmus53*/pc2G-FW. L, 1-kb DNA ladder; N, no-template control; PS, QM6a Δ*tmus53*; GF, QM6a Δ*tmus53* Δ*pyr4*/pc2G-FW; GR, QM6a Δ*tmus53* Δ*pyr4*/pc2G-RV; P, QM6a Δ*tmus53* Δ*pyr4*; PG, QM6a Δ*tmus53*/pc2G-FW.

fluorescence microscopy (Fig. 5). Notably, the transformed strains are prototrophic and ostensibly isogenic, besides containing the introduced gene of interest at the manipulated loci, compared to their parental strain.

**Construction of a double-auxotrophic *T. reesei* strain.** In particular with regard to metabolic engineering, there is a frequent need for multiple foreign gene insertions. To facilitate such a task, we constructed a *T. reesei* Δ*pyr4* Δ*asl1* strain. The transformation of QM6a Δ*tmus53*Δ*pyr4* with pCD-Δasl1 resulted in eight candidates (Δ*pyr4* Δ*asl1*), six of which were subjected to four rounds of homokaryon purification via streaking of conidial spores. One ʟ-arginine auxotrophic strain was obtained and tested for integration of the hygromycin resistance cassette into the *asl1* locus by PCR followed by sequencing of the PCR products (data not shown). Exclusive integration of the deletion cassette into the correct locus was verified by Southern blotting (Fig. 2D). The obtained strain is uridine and ʟ-arginine auxotrophic (Fig. 4, Δ*pyr4* Δ*asl1* strain). This strain can be used as a recipient strain for two independent gene insertions, again yielding a strain which is ostensibly isogenic and prototrophic. During metabolic engineering, it is likely that the expression of more than one foreign gene is desired, which is facilitated by using the Δ*pyr4* Δ*asl1* strain. It even spares the possibility of using other frequently used marker genes (such as *hyg* or *amdS*) for further rounds of strain engineering.

**Orientation and transformation strategy influence the expression of an inserted gene.** We were interested in whether the orientation and/or the transformation strategy used influences the expression of the inserted gene, as the proposed transformation procedure is in particular recommended for gene insertion with the aim of strain engineering. For this investigation, we used two transformation strategies, namely, the deletion of *pyr4* and reestablishment of *pyr4*, for the integration of the *A. niger goxA* gene
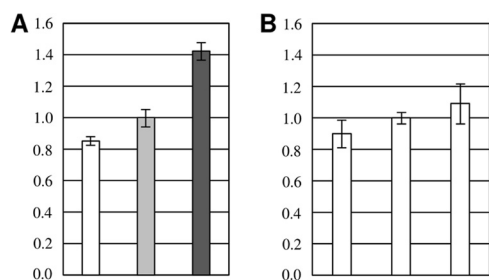
**FIG 7** Comparison of *goxA* expression depending on transformation strategy and orientation. (A) *T. reesei* strains QM6a Δ*tmus53*/pc2G-FW (white bar), QM6a Δ*tmus53* Δ*pyr4*/pc2G-FW (light gray bar), and QM6a Δ*tmus53* Δ*pyr4*/pc2G-RV (dark gray bar) were precultured on glycerol and transferred to sophorose for 8 h. Glucose oxidase activity in supernatants was measured and normalized to the biomass (dry weight). Values are means from biological duplicates and technical triplicates and are given as fold changes (*y* axes) comparing the investigated strains (*x* axes). Error bars indicate standard deviations. (B) Three genetically identical *T. reesei* strains (QM6a Δ*tmus53*pc2G-FW) were analyzed in an analogous experiment.

## DISCUSSION

We identified *asl1* as a novel and highly distinct auxotrophic marker in *T. reesei*. Notably, small traces of L-arginine in the selection medium are necessary to obtain transformed strains with a reestablished *asl1* locus (see Materials and Methods). In addition to its function in the biosynthesis of L-arginine, the argininosuccinate lyase plays an important role in the central metabolism of *T. reesei*. We suppose that this might be the reason for the observed sharp discrimination. This could also explain the rather low number of transformants obtained, which is about 10-fold lower than with transformation using *hyg* as marker gene (a comparison of transformation strategies is given in Table 2). We speculate that transformed strains already need to be homokaryotic in order to be able to grow on minimal medium. This idea is supported by the fact that only one round of homokaryon selection was necessary to obtain genomically homogenous strains.

The transformation targeting the EYFP gene expression cassette into the *asl1* locus led exclusively to prototrophic strains, 100% of which turned out to be successfully transformed. We assume that this outstandingly high rate (a comparison of transformation strategies is given in Table 2) is based on the design of the split-marker system: only a part of *asl1* is used as the marker on the targeting plasmid. Therefore, prototrophy is regained only when the marker (with it the gene of interest) integrates at the *asl1* locus. The insertion of the EYFP gene upstream of *asl1* did not have any effect on growth and sporulation behavior, making this locus a suitable target for site-specific gene insertions.

In a similar way, this study demonstrated that the locus of the established marker *pyr4* can be used as a platform for site-specific integration. However, the integration rate using the *pyr4* locus was lower than that with *asl1* (Table 2). This might be due to the fact that a fully functional *pyr4* expression cassette was used for reestablishment of the locus, which was different from the case for *asl1*. Hence, in the case of *pyr4*, prototrophy can also be regained by integration of the marker elsewhere in the genome. However, this property spares the possibility of using *pyr4* as a marker for integration events outside the locus (e.g., gene deletions) in the presented strains.

The observed semiauxotrophy of the Δ*hah1* strain could be explained in three ways. First, the annotation of the gene could be wrong. However, this is in our opinion rather unlikely, as the conserved domain search on http://www.ncbi.nlm.nih.gov/Structure/cdd/wrpsb.cgi predicts the protein to be a homoaconitase with an E value of 0e+00. Given that the function of the gene is correctly predicted, the second obvious explanation is that another (un-

fused to the *cbh2* promoter in two directions. A schematic presentation of the three types of strain constructions is provided in Fig. 6A to C. The correct and exclusive integration of *goxA* into the *pyr4* locus was verified by PCR and subsequent sequencing (Fig. 6D and E) as well as by Southern blotting (Fig. 6F). GoxA was chosen for easy monitoring and comparison of gene expression. The strains were precultured on glycerol and then transferred to sophorose (inducing condition) and incubated for 5 and 8 h. Afterwards, glucose oxidase activity in supernatants was determined by an enzymatic assay. We could detect no differences between the strains after 5 h of incubation (data not shown). However, we found that the *goxA* expression was higher in a *pyr4* deletion background (QM6a Δ*tmus53* Δ*pyr4*/pc2G-FW) than in a strain in which *pyr4* was reestablished (QM6a Δ*tmus53*/pc2G-FW) after 8 h of incubation (Fig. 7A). Notably, the *goxA* expression differed even more strongly between strains bearing the inserted construct in different orientations but obtained by the same transformation strategy (namely, *pyr4* deletion) (compare QM6a Δ*tmus53* Δ*pyr4*/pc2G-FW and QM6a Δ*tmus53* Δ*pyr4*/pc2G-RV in Fig. 7A). In a second experiment, we analogously analyzed the *goxA* expression in three strains with an identical genetic background (QM6a Δ*tmus53*/pc2G-FW) and found no significant differences in the reporter expression (Fig. 7B). This result highlights the need for targeted gene insertion in order to obtain strains that are accurately comparable concerning heterologous gene expression levels.

**TABLE 2** Comparison of transformation strategies

| Transformation strategy | No. of protoplasts used | Amt of linearized DNA used (µg) | No. of transformants obtained (mean ± SD) | Rate of positive transformants (%, mean ± SD) |
|---|---|---|---|---|
| Gene deletions using *hyg* as marker[a] | $10^7$ | 30 | 20 ± 2 | 63 ± 12 |
| Gene integration using split marker[b] | $10^7$ | 50 | 3 ± 1 | 100 |
| Gene integration using full-length marker[c] | $10^7$ | 50 | 4 ± 1 | 86 ± 7 |
| Ectopic gene integration (cotransformation)[d] | $10^7$ | 5 (target gene) and 1 (marker gene)[e] | 48 ± 12 | 76 ± 14 |

[a] Deletion of *asl1* and *hah1* in this study.
[b] Integration of the EYFP gene upstream of *asl1* using a partial *asl1* expression cassette as the marker in this study.
[c] Integration of the EYFP gene upstream of *pyr4* using a full-length *pyr4* expression cassette as the marker in this study.
[d] Average results from our laboratory.
[e] Circular plasmids were used.

known) enzyme can replace the Hah1 activity or that the organism is able to bypass this reaction. Third, and most likely, *T. reesei* might be able to store L-lysine in vast amounts in its vacuoles and could reuse the stored compound in case of L-lysine shortage. This behavior was already observed and described for *Saccharomyces cerevisiae* (37). If this is also true for *T. reesei*, it is generally not possible to use genes coding for enzymes involved in L-lysine biosynthesis as markers for *Trichoderma* transformation.

Finally, we recommend the use of the constructed L-arginine/uridine double-auxotrophic strain for advanced metabolic strain engineering. It represents an attractive host for insertion of multiple genes or a sequence of insertion and deletion without the necessity for marker recycling. It should be noted that the hygromycin resistance is lost upon reestablishment of the *asl1* locus and, therefore, is again available for an additional manipulation step, in both the double mutant and the L-arginine auxotrophic strain. However, besides this, another important observation was made during this study: the assessment of the importance of the orientation of an inserted gene and the applied transformation strategy (i.e., the final locus) revealed that both influence target gene expression. Notably, the impact of gene orientation was more pronounced than that of the locus. Even though there are only rare reports on the influence of the orientation of a gene on its expression, some studies carried out with organisms of other kingdoms found indications for the importance of gene orientation. For example, in mammalian cells, the orientation of a construct influenced the position effect with respect to chromatin (38). Another study with maize plants provided evidence that gene expression can be impacted by altering the orientation of adjacent genes (39). Obviously, this aspect also needs to be considered during strain engineering in *T. reesei*.

## ACKNOWLEDGMENTS

## REFERENCES

1. **Kuhls K, Lieckfeldt E, Samuels GJ, Kovacs W, Meyer W, Petrini O, Gams W, Börner T, Kubicek CP.** 1996. Molecular evidence that the asexual industrial fungus *Trichoderma reesei* is a clonal derivative of the ascomycete *Hypocrea jecorina*. Proc Natl Acad Sci U S A **93:**7755–7760. http://dx.doi.org/10.1073/pnas.93.15.7755.
2. **Teeri T, Salovuori I, Knowles J.** 1983. The molecular cloning of the major cellulase gene from *Trichoderma reesei*. Biotechnology **1:**696–699. http://dx.doi.org/10.1038/nbt1083-696.
3. **Kubicek CP, Harman GE.** 1998. *Trichoderma* and *Gliocladium*. Taylor & Francis, London, United Kingdom.
4. **Kumar R, Singh S, Singh OV.** 2008. Bioconversion of lignocellulosic biomass: biochemical and molecular perspectives. J Ind Microbiol Biotechnol **35:**377–391. http://dx.doi.org/10.1007/s10295-008-0327-8.
5. **Cherry JR, Fidantsef AL.** 2003. Directed evolution of industrial enzymes: an update. Curr Opin Biotechnol **14:**438–443. http://dx.doi.org/10.1016/S0958-1669(03)00099-5.
6. **Strauss J, Mach RL, Zeilinger S, Hartler G, Stöffler G, Wolschek M, Kubicek CP.** 1995. Cre1, the carbon catabolite repressor protein from *Trichoderma reesei*. FEBS Lett **376:**103–107. http://dx.doi.org/10.1016/0014-5793(95)01255-5.
7. **Saloheimo A, Aro N, Ilmén M, Penttilä M.** 2000. Isolation of the *ace1* gene encoding a Cys(2)-His(2) transcription factor involved in regulation of activity of the cellulase promoter cbh1 of *Trichoderma reesei*. J Biol Chem **275:**5817–5825. http://dx.doi.org/10.1074/jbc.275.8.5817.
8. **Aro N, Saloheimo A, Ilmén M, Penttilä M.** 2001. ACEII, a novel transcriptional activator involved in regulation of cellulase and xylanase genes of *Trichoderma reesei*. J Biol Chem **276:**24309–24314. http://dx.doi.org/10.1074/jbc.M003624200.
9. **Zeilinger S, Ebner A, Marosits T, Mach R, Kubicek C.** 2001. The *Hypocrea jecorina* HAP 2/3/5 protein complex binds to the inverted CCAAT-box (ATTGG) within the *cbh2* (cellobiohydrolase II-gene) activating element. Mol Genet Genomics **266:**56–63. http://dx.doi.org/10.1007/s004380100518.
10. **Rauscher R, Würleitner E, Wacenovsky C, Aro N, Stricker AR, Zeilinger S, Kubicek CP, Penttilä M, Mach RL.** 2006. Transcriptional regulation of *xyn1*, encoding xylanase I, in *Hypocrea jecorina*. Eukaryot Cell **5:**447–456. http://dx.doi.org/10.1128/EC.5.3.447-456.2006.
11. **Mach-Aigner AR, Grosstessner-Hain K, Poças-Fonseca MJ, Mechtler K, Mach RL.** 2010. From an electrophoretic mobility shift assay to isolated transcription factors: a fast genomic-proteomic approach. BMC Genomics **11:**644. http://dx.doi.org/10.1186/1471-2164-11-644.
12. **Seiboth B, Karimi RA, Phatale PA, Linke R, Hartl L, Sauer DG, Smith KM, Baker SE, Freitag M, Kubicek CP.** 2012. The putative protein methyltransferase LAE1 controls cellulase gene expression in *Trichoderma reesei*. Mol Microbiol **84:**1150–1164. http://dx.doi.org/10.1111/j.1365-2958.2012.08083.x.
13. **Häkkinen M, Valkonen MJ, Westerholm-Parvinen A, Aro N, Arvas M, Vitikainen M, Penttilä M, Saloheimo M, Pakula TM.** 2014. Screening of candidate regulators for cellulase and hemicellulase production in *Trichoderma reesei* and identification of a factor essential for cellulase production. Biotechnol Biofuels **7:**14. http://dx.doi.org/10.1186/1754-6834-7-14.
14. **Saloheimo M, Pakula TM.** 2012. The cargo and the transport system: secreted proteins and protein secretion in *Trichoderma reesei* (*Hypocrea jecorina*). Microbiology **158:**46–57. http://dx.doi.org/10.1099/mic.0.053132-0.
15. **Seidl V, Seibel C, Kubicek CP, Schmoll M.** 2009. Sexual development in the industrial workhorse *Trichoderma reesei*. Proc Natl Acad Sci U S A **106:**13909–13914. http://dx.doi.org/10.1073/pnas.0904936106.
16. **Tisch D, Schmoll M.** 2013. Targets of light signalling in *Trichoderma reesei*. BMC Genomics **14:**657. http://dx.doi.org/10.1186/1471-2164-14-657.
17. **Penttilä M, Nevalainen H, Rättö M, Salminen E, Knowles J.** 1987. A versatile transformation system for the cellulolytic filamentous fungus *Trichoderma reesei*. Gene **61:**155–164. http://dx.doi.org/10.1016/0378-1119(87)90110-7.
18. **Lorito M, Hayes CK, Di Pietro A, Harman GE.** 1993. Biolistic transformation of *Trichoderma harzianum* and *Gliocladium virens* using plasmid and genomic DNA. Curr Genet **24:**349–356. http://dx.doi.org/10.1007/BF00336788.
19. **Schuster A, Bruno KS, Collett JR, Baker SE, Seiboth B, Kubicek CP, Schmoll M.** 2012. A versatile toolkit for high throughput functional genomics with *Trichoderma reesei*. Biotechnol Biofuels **5:**1. http://dx.doi.org/10.1186/1754-6834-5-1.
20. **De Groot MJ, Bundock P, Hooykaas PJ, Beijersbergen AG.** 1998. *Agrobacterium* tumefaciens-mediated transformation of filamentous fungi. Nat Biotechnol **16:**839–842. http://dx.doi.org/10.1038/nbt0998-839.
21. **Steiger MG, Vitikainen M, Uskonen P, Brunner K, Adam G, Pakula T, Penttilä M, Saloheimo M, Mach RL, Mach-Aigner AR.** 2011. Transformation system for *Hypocrea jecorina* (*Trichoderma reesei*) that favors homologous integration and employs reusable bidirectionally selectable markers. Appl Environ Microbiol **77:**114–121. http://dx.doi.org/10.1128/AEM.02100-10.
22. **Gatignol A, Durand H, Tiraby G.** 1988. Bleomycin resistance conferred by a drug-binding protein. FEBS Lett **230:**171–175. http://dx.doi.org/10.1016/0014-5793(88)80665-3.
23. **Peterbauer CK, Heidenreich E, Baker RT, Kubicek CP.** 1992. Effect of benomyl and benomyl resistance on cellulase formation by *Trichoderma reesei* and *Trichoderma harzianum*. Can J Microbiol **38:**1292–1297. http://dx.doi.org/10.1139/m92-213.
24. **Kubodera T, Yamashita N, Nishimura A.** 2002. Transformation of *Aspergillus* sp. and *Trichoderma reesei* using the pyrithiamine resistance gene (*ptrA*) of *Aspergillus oryzae*. Biosci Biotechnol Biochem **66:**404–406. http://dx.doi.org/10.1271/bbb.66.404.

25. **Bergès T, Barreau C, Peberdy JF, Boddy LM.** 1993. Cloning of an *Aspergillus niger* invertase gene by expression in *Trichoderma reesei*. Curr Genet **24:**53–59. http://dx.doi.org/10.1007/BF00324665.

26. **Jørgensen M, Skovlund D, Johannesen P, Mortensen UH.** 2014. A novel platform for heterologous gene expression in *Trichoderma reesei* (teleomorph *Hypocrea jecorina*). Microb Cell Fact **13:**33. http://dx.doi.org/10.1186/1475-2859-13-33.

27. **Hartl L, Seiboth B.** 2005. Sequential gene deletions in *Hypocrea jecorina* using a single blaster cassette. Curr Genet **48:**204–211. http://dx.doi.org/10.1007/s00294-005-0011-8.

28. **Mach RL, Schindler M, Kubicek CP.** 1994. Transformation of *Trichoderma reesei* based on hygromycin B resistance using homologous expression signals. Curr Genet **25:**567–570. http://dx.doi.org/10.1007/BF00351679.

29. **Gruber F, Visser J, Kubicek CP, de Graaff LH.** 1990. The development of a heterologous transformation system for the cellulolytic fungus *Trichoderma reesei* based on a *pyrG*-negative mutant strain. Curr Genet **18:**71–76. http://dx.doi.org/10.1007/BF00321118.

30. **Debets AJ, Swart K, Holub EF, Goosen T, Bos CJ.** 1990. Genetic analysis of *amdS* transformants of *Aspergillus niger* and their use in chromosome mapping. Mol Gen Genet **222:**284–290. http://dx.doi.org/10.1007/BF00633830.

31. **Mandels M.** 1985. Applications of cellulases. Biochem Soc Trans **13:**414–416.

32. **Druzhinina IS, Schmoll M, Seiboth B, Kubicek CP.** 2006. Global carbon utilization profiles of wild-type, mutant, and transformant strains of *Hypocrea jecorina*. Appl Environ Microbiol **72:**2126–2133. http://dx.doi.org/10.1128/AEM.72.3.2126-2133.2006.

33. **Hickey PC, Read ND.** 2009. Imaging living cells of *Aspergillus* in vitro. Med Mycol **47**(Suppl 1):S110–S119. http://dx.doi.org/10.1080/13693780802546541.

34. **Mach RL, Peterbauer CK, Payer K, Jaksits S, Woo SL, Zeilinger S, Kullnig CM, Lorito M, Kubicek CP.** 1999. Expression of two major chitinase genes of *Trichoderma atroviride* (*T. harzianum* P1) is triggered by different regulatory signals. Appl Environ Microbiol **65:**1858–1863.

35. **Swart K, Debets AJ, Kobus G, Bos CJ.** 1992. Arginine and proline genes of *Aspergillus niger*. Antonie Van Leeuwenhoek **61:**259–264. http://dx.doi.org/10.1007/BF00713933.

36. **Weidner G, Steffan B, Brakhage AA.** 1997. The *Aspergillus nidulans lysF* gene encodes homoaconitase, an enzyme involved in the fungus-specific lysine biosynthesis pathway. Mol Gen Genet **255:**237–247. http://dx.doi.org/10.1007/s004380050494.

37. **Kitamoto K, Yoshizawa K, Ohsumi Y, Anraku Y.** 1988. Dynamic aspects of vacuolar and cytosolic amino acid pools of *Saccharomyces cerevisiae*. J Bacteriol **170:**2683–2686.

38. **Feng YQ, Lorincz MC, Fiering S, Greally JM, Bouhassira EE.** 2001. Position effects are influenced by the orientation of a transgene with respect to flanking chromatin. Mol Cell Biol **21:**298–309. http://dx.doi.org/10.1128/MCB.21.1.298-309.2001.

39. **Unger E, Betz S, Xu R, Cigan AM.** 2001. Selection and orientation of adjacent genes influences DAM-mediated male sterility in transformed maize. Transgenic Res **10:**409–422. http://dx.doi.org/10.1023/A:1012032000383.